

On accuracy of the mass-preserving DG method to multi-dimensional Schrödinger equations

HAILIANG LIU*

Mathematics Department, Iowa State University, Ames, IA 50011, USA

*Corresponding author: hliu@iastate.edu

YUNQING HUANG

Hunan Key Laboratory for Computation and Simulation in Science and Engineering,

School of Mathematics and Computational Science, Xiangtan University,

Xiangtan 411105, People's Republic of China

WENYING LU

School of Mathematics and Computational Science, Hunan University of Science and Technology,

Xiangtan 411201, People's Republic of China

wylu@hnust.edu.cn

AND

NIANYU YI*

Hunan Key Laboratory for Computation and Simulation in Science and Engineering,

School of Mathematics and Computational Science, Xiangtan University,

Xiangtan 411105, People's Republic of China

*Corresponding author: yinanyu@xtu.edu.cn

[Received on 21 July 2016; revised on 13 August 2017]

In this paper, we present two approaches to the error analysis of a semidiscrete mass-preserving discontinuous Galerkin method, introduced by Lu, Huang and Liu (2015, Mass preserving direct discontinuous Galerkin methods for Schrödinger equations. *J. Comp. Phys.*, **282**, 210–226), for the solution of multi-dimensional Schrödinger equations. The first approach is based on an explicit global projection using tensor product polynomials on rectangular meshes. The L^2 error bound obtained is optimal, independent of the size of the flux parameter. The second approach is based on an implicit global projection using standard polynomials on arbitrary shape-regular meshes. The L^2 error bound obtained for this method is also optimal, but it is valid only when the flux parameter is sufficiently large. Numerical experiments are presented to demonstrate the theoretical results.

Keywords: DG method; Schrödinger equation; numerical flux; global projection; superconvergence.

1. Introduction

In this paper we prove the optimal L^2 error estimates of the mass-preserving discontinuous Galerkin (MPDG) method for solving linear Schrödinger equations,

$$iu_t + \Delta u - \Phi(x)u = 0, \quad (x, t) \in \Omega \times [0, T], \quad (1.1a)$$

$$u(x, 0) = u_0(x), \quad (1.1b)$$

where Ω is a bounded rectangular domain in \mathbb{R}^d , $u_0(x)$ is a given smooth complex function and Φ is a real smooth potential function. We assume periodic boundary conditions for simplicity, although this is not essential for the analysis; other boundary conditions can also be considered along the same lines.

The MPDG method studied here was introduced in the study by [Lu et al. \(2015\)](#) for solving both linear and nonlinear Schrödinger equations. As for the semidiscrete MPDG method in one-dimensional setting, the optimal L^2 error estimates was obtained in [Lu et al. \(2015\)](#). The key idea, following [Liu \(2015\)](#) and [Liu & Ploymaklam \(2015\)](#), was to introduce a global L^2 projection dictated by the choice of numerical fluxes, with which the troublesome terms are eliminated in the error equation, leading therefore to optimal L^2 error estimates. However, such a technique is no longer directly applicable in the multi-dimensional setting.

Our main objective in this work is to obtain optimal L^2 error estimates for semidiscrete MPDG schemes in solving (1.1). We present two different approaches to handle both structured and unstructured meshes. The first approach is a direct extension of the analysis in the study by [Lu et al. \(2015\)](#) based on the tensor product of polynomials for rectangular meshes, yet the troublesome terms from interfaces cannot be completely eliminated in the multi-dimensional case. A superconvergence result is established by taking advantage of the Cartesian structure of the grid; using this superconvergence result we are able to obtain the optimal L^2 error estimate. Moreover, the obtained result is valid with or without a flux parameter.

The second approach is to handle unstructured shape-regular meshes. The semidiscrete MPDG scheme with penalty using standard polynomials is shown to admit the optimal L^2 error estimate. Here we follow some error estimate techniques in the discontinuous Galerkin (DG) method for elliptic problems (see [Arnold et al., 2002](#)). The main novelty is the global projection defined by

$$\int_{\Omega} (u - \Pi u)v \, dx + A(u - \Pi u, v) = 0,$$

for cell-wise polynomials v and the corresponding global bilinear operator $A(\cdot, \cdot)$. The existence of such a projection and the corresponding projection error are obtained by using the coercivity property of the bilinear operator $A(\cdot, \cdot)$. In the analysis of the projection error both the energy error and the L^2 error are carefully derived through two coupled inequalities. For the MPDG approximation we split the error between the exact solution u and the numerical solution u_h into two parts: $u_h - \Pi u$ and $\Pi u - u$, which enables us to control both cell integrals and the inter-element jump terms simultaneously. The obtained result is shown to be valid only when the flux parameter is suitably large, even though MPDG methods also give an optimal convergence rate in numerical tests for β small or zero.

In the study by [Xu & Shu \(2005\)](#), a local discontinuous Galerkin (LDG) method was developed to solve the generalized nonlinear Schrödinger equation. For the linearized Schrödinger equation, the authors proved the error estimate of order $k + 1/2$ for polynomials of degree k . The optimal error estimate was further verified in the study by [Xu & Shu \(2012\)](#) by using special local projections. In the study by [Lu et al. \(2004\)](#), an LDG method was presented for solving one-dimensional linear Schrödinger equations so that the mass is preserved numerically. In the study by [Zhang et al. \(2012a\)](#), a mass-preserving DG method was presented for the one-dimensional coupled nonlinear Schrödinger equation, and in the study by [Zhang et al. \(2012b\)](#) for both one- and two-dimensional nonlinear Schrödinger equations. In the studies by [Zhang et al. \(2012a,b\)](#), the authors adopted a numerical flux for the solution gradient as the diffusive flux proposed in the study by [Liu & Yan \(2010\)](#).

In the study by *Zhang et al.* (2012b) the conservation property is verified, and further validated by some long-time simulation results.

For simulating solutions of Schrödinger equations, both linear and nonlinear, various kinds of numerical methods can be found in the literature. For instance, the finite difference method (*Delfour et al.*, 1981; *Taha & Ablowitz*, 1984; *Chang & Xu*, 1986; *Chang & Wang*, 1990; *Chang et al.*, 1999; *Kurtinaitis & Ivanauskas*, 2004; *Becerril et al.*, 2008), the finite element method (*Levin & Shertzer*, 1985; *Chang & Wang*, 1990; *Robinson*, 1991; *Karakashian & Makridakis*, 1998), the spectral method (*Feit et al.*, 1982; *Feit & Fleck*, 1983; *Hermann & Fleck*, 1988; *Pathria & Morris*, 1990) and the splitting method (*Bao et al.*, 2002; *Gradinaru*, 2007). The MPDG method falls into the category of direct DG (DDG) methods for higher-order PDEs, as introduced in the studies by *Liu & Yan* (2009, 2010) for diffusion. The feature in the DDG schemes proposed in the studies by *Liu & Yan* (2009, 2010) lies in numerical flux choices for the solution gradient, which involve higher-order derivatives evaluated when crossing interfaces, motivated by a trace formula for the derivatives of the heat solution (see *Liu & Yan*, 2009). With this choice, the schemes obtained are provably stable and optimally convergent (*Liu*, 2015). In contrast, the numerical flux for the solution gradient in the MPDG method (*Lu et al.*, 2015) to Schrödinger equations is much simpler, clearly indicating that the MPDG method provides an attractive alternative for solving the Schrödinger equations.

Obtaining *a priori* error estimates for various DG methods has been a major subject of research. In the literature, there are only a few works on error estimates of the DG method for higher-order PDEs, while the main technical difficulty in obtaining an optimal error estimate lies in the lack of control of jump terms on cell interfaces. The first *a priori* error estimate of order $\mathcal{O}(h^k)$ for the LDG method of linear convection–diffusion was obtained in the study by *Cockburn & Shu* (1998). With a particular numerical flux, the optimal convergence rate of order $\mathcal{O}(h^{k+1})$ was obtained in the studies by *Castillo* (2000) and *Castillo et al.* (2000, 2002). For the numerical method of *Baumann & Oden* (1999) when applied to nonlinear convection–diffusion equations, the optimal error estimate for at least quadratic polynomials was obtained by *Rivière & Wheeler* (2000). For the DDG method, the first *a priori* error estimate of order $\mathcal{O}(h^k)$ for linear diffusion was obtained in the study by *Liu & Yan* (2010). The optimal order is further obtained in the study by *Liu* (2015) by the use of a global projection, which eliminates troublesome jump terms in the error equation and allows for an effective control of nonlinear convection with the aid of numerical dissipation and projection error bounds. The error analysis using a global projection also applies well to conservative DG methods for dispersive PDEs, for instance in the study by *Bona et al.* (2013) for the generalized Korteweg–de Vries (KdV) equation, in the study by *Liu & Ploymaklam* (2015) for the Burgers–Poisson system and in the study by *Liu & Yi* (2016) for a Hamiltonian-preserving DG method for the generalized KdV equation.

The rest of the paper is organized as follows: in Section 2, we review the semidiscrete MPDG method for the one-dimensional Schrödinger equation (1.1), and the optimal L^2 error estimate result. In Section 3, we investigate the MPDG method with rectangular meshes. The error estimate of the semidiscrete MPDG method for solving (1.1) is presented, while an explicit global projection plays a special role. For unstructured shape-regular meshes, we prove the optimal L^2 error estimate for the MPDG method with penalty (large flux parameter β) in Section 4. We provide numerical examples to show our theoretical results in Section 5. Finally, concluding remarks are given in Section 6.

Notation. Throughout the paper we denote the L^2 -norm by $\|\cdot\|$, the L^∞ -norm by $\|\cdot\|_\infty$, the H^m -norm by $\|\cdot\|_m$ and the H^m -seminorm by $|\cdot|_m$. $W^{m,p}$ with $1 \leq p \leq \infty$ as the usual Sobolev space, with $W^{m,2} = H^m$. We may specify the integral domain explicitly if it is a computational cell I_j or K , or a master domain $\hat{I} := [-1, 1]$. If it is the whole domain Ω , we do not specify the domain unless necessary. We also denote by $\partial\Omega$ the boundary of Ω .

2. The MPDG method for one-dimensional Schrödinger equations

In this section, we review the MPDG method for the one-dimensional problem

$$iu_t + u_{xx} - \Phi(x)u = 0, \quad (2.1)$$

subject to initial data

$$u(x, 0) = u_0(x) \quad (2.2)$$

imposed on $\Omega = [0, L]$, with periodic boundary conditions.

Let the mesh be $I_j = [x_{j-\frac{1}{2}}, x_{j+\frac{1}{2}}]$ for $j = 1, 2, \dots, N$. The center of the cell is $x_j = (x_{j-\frac{1}{2}} + x_{j+\frac{1}{2}})/2$ and $h_j = x_{j+\frac{1}{2}} - x_{j-\frac{1}{2}}$. We denote the complex piecewise polynomial space V_h as the space of polynomials of degree at most k in each cell I_j , i.e.,

$$V_h := \{v : v \in P^k(I_j), \quad j = 1, 2, \dots, N\}.$$

Then the semidiscrete DDG scheme of (2.1) is as follows: find $u_h \in V_h$ such that

$$i \int_{I_j} u_{ht} v \, dx - \int_{I_j} u_{hx} v_x \, dx + \widehat{u}_{hx} v \Big|_{j-\frac{1}{2}}^{j+\frac{1}{2}} + (u_h - \widehat{u}_h) v_x \Big|_{j-\frac{1}{2}}^{j+\frac{1}{2}} - \int_{I_j} \Phi u_h v \, dx = 0 \quad (2.3)$$

holds for $\forall v \in V_h$, where

$$w \Big|_{j-\frac{1}{2}}^{j+\frac{1}{2}} = w(x_{j+1/2}^-) - w(x_{j-1/2}^+),$$

and the numerical fluxes are

$$\widehat{u}_{hx} = \beta \frac{[u_h]}{h} + \theta u_{hx}^+ + (1 - \theta) u_{hx}^-, \quad \widehat{u}_h = (1 - \theta) u_h^+ + \theta u_h^-, \quad \forall \theta \in [0, 1], \quad (2.4)$$

where $h = \frac{1}{2}(\Delta x_{j+1} + \Delta x_j)$ and $[w] = w(x_{j+1/2}^+) - w(x_{j+1/2}^-)$ when evaluated at the cell interface $x_{j+1/2}$. The parameter β is a real number to be selected to tune the scheme for achieving optimal convergence. At the domain boundary we use a periodic extension to determine the numerical flux.

In the study by Lu *et al.* (2015) a global projection $\mathcal{P}w$ on Ω is introduced so that $\mathcal{P}w|_{I_j} \in P^k(I_j)$ for $k \geq 1$ and $w \in C^1$, satisfying

$$\int_{I_j} (\mathcal{P}w - w) v \, dx = 0 \quad \forall v \in P^{k-2}(I_j), \quad j = 1, \dots, N \quad (2.5)$$

and

$$\widehat{\mathcal{P}w}|_{j+\frac{1}{2}} = w\left(x_{j+\frac{1}{2}}\right), \quad \widehat{\mathcal{P}w}_x|_{j+\frac{1}{2}} = w_x\left(x_{j+\frac{1}{2}}\right), \quad j = 1, \dots, N, \quad (2.6)$$

where

$$\widehat{\mathcal{P}w} := (1 - \theta)\mathcal{P}w^+ + \theta\mathcal{P}w^-, \quad \widehat{\mathcal{P}w}_x := \frac{\beta [\mathcal{P}w]}{h} + \theta\mathcal{P}w_x^+ + (1 - \theta)\mathcal{P}w_x^-. \quad (2.7)$$

Note that for $k = 1$, instead of (2.5), we need only (2.6) to define the unique projection. At the domain boundary the periodic extension is adopted to be consistent with the selected numerical flux. For a piecewise smooth function w , we need to replace $w(x_{j+\frac{1}{2}})$ by $\widehat{w}|_{x_{j+\frac{1}{2}}}$, and $w_x(x_{j+\frac{1}{2}})$ by $\widehat{w}_x|_{x_{j+\frac{1}{2}}}$, respectively. Hence the error estimate between the exact solution U and the numerical solution u can be estimated as

$$\|u_h - u\| \leq \|u_h - \mathcal{P}u\| + \|u - \mathcal{P}u\|. \quad (2.8)$$

With this global projection the troublesome terms in the error equation are under control, so that it is possible to recover the optimal estimate, as long as the projection is well defined and has the desired approximation properties. Indeed, the following was established in the study by Lu *et al.* (2015). We observe that a more refined condition for k is necessary for the general case, so we revisit the proof by showing the places where the condition is refined.

LEMMA 2.1 The projection \mathcal{P} is uniquely defined for

$$\beta \neq 2k\theta(1-\theta)\cos(k+1+2j/N)\pi + k^2\left(\theta^2 + (1-\theta)^2\right), \quad j = 0, \dots, N-1, \quad (2.9)$$

if $\theta \in (0, 1)$, or for any real β if $\theta = 0$ or $\theta = 1$.

Proof. The global projection $\mathcal{P}w$ may be expressed as

$$\mathcal{P}w(x)|_{I_j} = \sum_{l=1}^{k+1} c_l^j \varphi_l(\xi), \quad \xi = \frac{x - x_j}{h_j/2}, \quad j = 1, \dots, N, \quad (2.10)$$

where $\{\varphi_l\}_1^{k+1}$ is the Legendre basis, which is a sequence of orthogonal polynomials on $[-1, 1]$. Equation (2.5) and the orthogonality of the Legendre polynomials imply that one may take $v = \varphi_i$ to get

$$c_i^j = \frac{2i-1}{2} \int_{-1}^1 w\left(x_j + \frac{h_j}{2}\xi\right) \varphi_i(\xi) d\xi, \quad i = 1, \dots, k-1, \quad (2.11)$$

where we have used $\int_{-1}^1 \varphi_i^2(\xi) d\xi = \frac{2}{2i-1}$. It remains to determine both c_k^j and c_{k+1}^j , $j = 1, \dots, N$. Condition (2.6) gives

$$\begin{cases} \theta \sum_{l=1}^{k+1} c_l^j \varphi_l(1) + (1-\theta) \sum_{l=1}^{k+1} c_l^{j+1} \varphi_l(-1) = w\left(x_{j+\frac{1}{2}}\right), \\ -\beta \sum_{l=1}^{k+1} c_l^j \varphi_l(1) + \beta \sum_{l=1}^{k+1} c_l^{j+1} \varphi_l(-1) + 2(1-\theta) \sum_{l=1}^{k+1} c_l^j \varphi_l'(1) + 2\theta \sum_{l=1}^{k+1} c_l^{j+1} \varphi_l'(-1) = h_j w_x\left(x_{j+\frac{1}{2}}\right). \end{cases} \quad (2.12)$$

Using the periodic boundary condition, the matrix form of equation (2.12) reduces to

$$D \vec{c} = \vec{b}, \quad (2.13)$$

where $\vec{c}^j = (c^j), \vec{b}^j = (b^j)$, with

$$c^j = \begin{bmatrix} c_k^j \\ c_{k+1}^j \end{bmatrix}, \quad b^j = \begin{bmatrix} b_1^j \\ b_2^j \end{bmatrix} \quad (2.14)$$

$$= \begin{bmatrix} w(x_{j+1/2}) - (1-\theta) \sum_{l=1}^{k-1} c_l^{j+1} \varphi_l(-1) - \theta \sum_{l=1}^{k-1} c_l^j \varphi_l(1) \\ h_j w_x(x_{j+\frac{1}{2}}) - 2(1-\theta) \sum_{l=1}^{k-1} c_l^j \varphi_l'(1) - 2\theta \sum_{l=1}^{k-1} c_l^{j+1} \varphi_l'(-1) + \beta \sum_{l=1}^{k-1} c_l^j \varphi_l(1) - \beta \sum_{l=1}^{k-1} c_l^{j+1} \varphi_l(-1) \end{bmatrix},$$

for $j = 1, \dots, N$. The coefficient matrix D is

$$D = \begin{pmatrix} A & B & 0 & \cdots & \cdots & 0 \\ 0 & A & B & 0 & \cdots & 0 \\ \vdots & \ddots & \ddots & \ddots & \vdots & \vdots \\ \vdots & \ddots & \ddots & \ddots & A & B \\ B & \cdots & \cdots & \cdots & \cdots & A \end{pmatrix}_{N \times N}, \quad (2.15)$$

where

$$A = \begin{pmatrix} \theta \varphi_k(1) & \theta \varphi_{k+1}(1) \\ -\beta \varphi_k(1) + 2(1-\theta) \varphi_k'(1) & -\beta \varphi_{k+1}(1) + 2(1-\theta) \varphi_{k+1}'(1) \end{pmatrix},$$

$$B = \begin{pmatrix} (1-\theta) \varphi_k(-1) & (1-\theta) \varphi_{k+1}(-1) \\ \beta \varphi_k(-1) + 2\theta \varphi_k'(-1) & \beta \varphi_{k+1}(-1) + 2\theta \varphi_{k+1}'(-1) \end{pmatrix}.$$

Recall that

$$\varphi_k(\pm 1) = (\pm 1)^{k-1}, \quad k = 1, 2, \dots, \quad \varphi_k'(\pm 1) = \frac{1}{2} (\pm 1)^k k(k-1), \quad k = 2, 3, \dots;$$

then a direct calculation shows

$$\det(A) = 2\theta(1-\theta) [\varphi_{k+1}'(-1) - \varphi_k'(-1)] = 2k\theta(1-\theta).$$

For $0 < \theta < 1$ and $k \geq 1$, A^{-1} exists; hence the determinant of D can be expressed as

$$\det(D) = |A|^N |I + (-1)^{N-1} (A^{-1} B)^N|.$$

We want to show $\det(D) \neq 0$. To this end, we let ω satisfy $|\omega| = 1$, and calculate

$$\begin{aligned} & \det \left(A + (-1)^{k-1} \omega B \right) \\ &= \begin{vmatrix} \theta + (1-\theta)\omega & \theta - (1-\theta)\omega \\ \beta(\omega-1) + k(k-1)(1-\theta-\theta\omega) & -\beta(\omega+1) + k(k+1)(1-\theta+\theta\omega) \end{vmatrix} \\ &= -2\omega \left(\beta - k \left[\theta(1-\theta)(\bar{\omega}+\omega) + k(\theta^2 + (1-\theta)^2) \right] \right). \end{aligned}$$

One can verify that $\det(D) = 0$ if and only if there exists λ such that

$$\lambda^N = (-1)^N,$$

where λ denotes an eigenvalue of $A^{-1}B$, which can be complex. For a fixed ω , if β is selected such that $\det(A + (-1)^{k-1} \omega B) = 0$, then we have $\lambda = (-1)^k/\omega$. We thus determine ω such that

$$\lambda^N = (-1)^{kN}/\omega^N = (-1)^N,$$

from which we must have

$$\omega = \exp(\pi(k+1+2j/N)i), \quad j = 0, 1, \dots, N-1.$$

Hence, in order for $\det(D) \neq 0$ to hold, it is sufficient to select

$$\beta \neq 2k\theta(1-\theta) \cos(k+1+2j/N)\pi + k^2(\theta^2 + (1-\theta)^2).$$

In addition, when $\theta = 0$ or 1 , (2.5)–(2.6) becomes a local projection, whose existence is similar but easier to verify. In a sentence, for any $\theta \in [0, 1]$, $\mathcal{P}w$ is uniquely defined with a proper choice of β as stated in (2.9). \square

REMARK 2.2 For $k \geq 2$, $\beta = 0$ suffices to ensure the existence of the projection for any $\theta \in [0, 1]$. For $\theta = \frac{1}{2}$, it suffices to choose $\beta \neq \frac{k}{2} [k + \cos(k+1+2j/N)\pi]$ for $j = 0, \dots, N-1$.

LEMMA 2.3 (Lu *et al.*, 2015). Assume that $w \in H^m$ with $m \geq k+1$. If the global projection is uniquely defined, then we have the projection error

$$\|w - \mathcal{P}w\| \leq Ch^{k+1} |w|_{k+1}, \quad (2.16)$$

where C is independent of h .

All these together lead to the following result.

THEOREM 2.4 (Lu *et al.*, 2015). The error between the exact solution u of (2.1) and the numerical solution u of (2.3), (2.4) with β satisfying (2.9) satisfies

$$\|u(\cdot, t) - u_h(\cdot, t)\| \leq Ch^{k+1}, \quad 0 < t \leq T, \quad (2.17)$$

where C depends on $|u|_{k+1}$, $|u_t|_{k+1}$, T and the data given, but is independent of h .

Numerical experiments carried out in the study by [Lu *et al.* \(2015\)](#) indicate that different choices of $\theta \in [0, 1]$ yield the same order of accuracy, though numerical errors can be slightly different. We also observed that both numerical errors and orders of convergence are identical for both $\theta = \alpha$ and $\theta = 1 - \alpha$ for $\alpha \in [0, 1]$. Therefore, in the error analysis presented in this work we restrict ourselves to the case $\theta = \frac{1}{2}$.

3. Error estimates for rectangular meshes

In this section we prove the optimal error estimates of MPDG approximation based on tensor-product polynomials of the multi-dimensional Schrödinger equation

$$iu_t + \Delta u = \Phi(x)u, \quad t > 0, \quad (3.1)$$

posed on $x = (x^1, \dots, x^d) \in \Omega = \prod_{i=1}^d [0, L_i] \subset \mathbb{R}^d$, subject to both initial data $u(x, 0) = u_0(x)$ and periodic boundary conditions. It is known from the study by [Jensen \(1986\)](#) that if $\Phi \in W^{m, \infty}(m \geq 0)$ is a real-valued function, then the solution operator maps from H^m to H^m for any $t > 0$. In our error estimate result, we will assume Φ has required regularity so that the solution has smoothness as needed in our error estimates.

3.1 Scheme formulation

We partition the domain Ω into rectangular meshes

$$\Omega = \bigcup_{\alpha=1}^N K_\alpha,$$

where $\alpha = (\alpha_1, \dots, \alpha_d)$, $N = (N_1, \dots, N_d)$. We use rectangular meshes $\{K\} \subset \mathcal{T}_h$, with $K_\alpha = I_{\alpha_1}^1 \times \dots \times I_{\alpha_d}^d$, where $I_{\alpha_i}^i = [x_{\alpha_i-1/2}^i, x_{\alpha_i+1/2}^i]$ for $\alpha_i = 1, \dots, N_i$. Denote by $h^i = \max_{1 \leq \alpha_i \leq N_i} |I_{\alpha_i}^i|$, with $h = \max_{1 \leq i \leq d} h^i$. In what follows we shall take uniform meshes with element size $\prod_{i=1}^d h^i$, unless otherwise stated.

We define the DG space as the space of tensor products of piecewise polynomials of degree at most k in each variable on every element, i.e.,

$$W_h = \{v : v \in Q^k(K_\alpha) \quad \forall x \in K_\alpha, \quad \alpha = 1, \dots, N\},$$

where Q^k is the space of tensor products of one-dimensional polynomials of degree up to k . For the one-dimensional case we have $Q^k(K) = P^k(K)$, which is the space of polynomials of degree at most k defined on K . Hence, the traces of functions in W_h are double valued on $\Gamma_h^0 := \Gamma_h \setminus \partial\Omega$ and single valued on $\Gamma_h^\partial = \partial\Omega$, where $\Gamma_h = \Gamma_h^0 \cup \Gamma_h^\partial$.

We also introduce some trace operators that will help us to define the interface terms. Let K^1 and K^2 be two neighboring cells with a common edge e ; for w defined on ∂K^i , $i = 1, 2$, we define the average $\{w\}$ and the jump $[w]$ as

$$\{w\} = \frac{1}{2}(w_1 + w_2), \quad [w] = w_2 - w_1 \quad \text{on } e,$$

where the jump is calculated as a forward difference along the normal direction \vec{n} , which is defined to be oriented from K^1 to K^2 , with $w_i = w|_{\partial K^i}$. We consider the DG scheme

$$i \int_{\Omega} u_{ht} v \, dx = A(u_h, v) + \int_{\Omega} \Phi(x) u_h v \, dx, \quad (3.2)$$

where

$$A(u_h, v) = \sum_{K \in \mathcal{T}_h} \int_K \nabla u_h \cdot \nabla v \, dx + \sum_{e \in \Gamma_h} \int_e (\widehat{\partial_n u_h}[v] + [u_h]\{\partial_n v\}) \, ds \quad (3.3)$$

with the numerical flux for $\partial_n u_h$ taken as

$$\widehat{\partial_n u_h} = \beta h_e^{-1} [u_h] + \{\partial_n u_h\}. \quad (3.4)$$

The characteristic length h for the edge $e = \partial K_1 \cap \partial K_2$ is typically defined as

$$h_e = |\overrightarrow{C_1 C_2} \cdot \vec{n}|, \quad (3.5)$$

where C_i is the centroid of element K_i , and \vec{n} is the unit vector normal to K_i . At the boundary we replace $\overrightarrow{C_1 C_2}$ by $2\overrightarrow{C_1 D}$ where $D \in e$ such that $\overrightarrow{C_1 D}$ is perpendicular to e . In the case of uniform rectangular meshes we have $h_e = h^i$ at each interface $x_{\alpha^i+1/2}^i$ for $\alpha_i = 1, \dots, N_i$. Note that in formulation (3.3), the choice of \vec{n} on the edge $e \in \Gamma_h^0$ (pointing to K_1 or K_2) does not affect the products $[u_h]\{\partial_n v\}$ and $\widehat{\partial_n u_h}[v]$. Hence, both $\{\partial_n u_h\}$ and $\{\partial_n v\}$ may be defined based on a fixed choice of \vec{n} on e . However, on $e \in \Gamma_h^\partial$, we take \vec{n} as the usual outside unit normal to $\partial\Omega \cap e$.

The initial data for the obtained semidiscrete DG scheme is given as

$$u_h = \Pi_0 u_0, \quad t = 0, \quad (3.6)$$

where Π_0 is the standard piecewise L_2 projection.

3.2 Conservation properties

We now discuss two important conservation properties of the above semidiscrete DG scheme. Note that for any $\beta \in \mathbb{R}$, the following holds:

$$A(v, v^*) = A(v^*, v), \quad (3.7)$$

where v^* denotes the complex conjugate of v . Therefore total mass is conserved in the sense that

$$\frac{d}{dt} \|u_h\|^2 = 0. \quad (3.8)$$

Furthermore, we choose $v = u_{ht}^*$, complex conjugate of u_{ht} , in (3.2), so that

$$i \int_{\Omega} |u_{ht}|^2 dx = A(u_h, u_{ht}^*) + \int_{\Omega} \Phi(x) u_h u_{ht}^* dx. \quad (3.9)$$

This, upon adding its conjugate, gives

$$\frac{d}{dt} \left(A(u_h, u_h^*) + \int_{\Omega} \Phi |u_h|^2 dx \right) = 0, \quad (3.10)$$

where

$$A(u_h, u_h^*) = \sum_{K \in \mathcal{T}_h} \int_K |\nabla u_h|^2 dx + \sum_{e \in \Gamma_h} \int_e (\beta h^{-1} |[u_h]|^2 + 2\operatorname{Re}(\{\partial_n u_h\} [u_h^*])) ds.$$

Hence, (3.10) may be regarded as the discrete approximation of the energy conservation

$$\frac{d}{dt} \int_{\Omega} (|\nabla u|^2 + \Phi(x) |u|^2) dx = 0,$$

which is another well-known feature of the Schrödinger equation.

3.3 Projection and projection properties

In order to obtain the estimate for the MPDG scheme (3.2), (3.3) and (3.4) with admissible β using rectangular meshes, we follow Liu (2015) to use an explicit global projection similar to the one-dimensional case. Such a projection can be defined as

$$\mathcal{P}w = \mathcal{P}^{(x^1)} \otimes \cdots \otimes \mathcal{P}^{(x^d)} w, \quad (3.11)$$

where the superscripts indicate the application of the one-dimensional operator $\mathcal{P}^{(x^i)}$ with respect to the corresponding variable x^i .

In other words, for a given (piecewise) smooth function w , the projection $\mathcal{P}w$ is the unique function in W_h defined in (3.11), with $P^{(x^i)}$ determined by

$$\int_{I_{\alpha_i}^i} \left(\mathcal{P}^{(x^i)} w(x) - w(x) \right) \partial_{x^i}^2 v(x) dx^i = 0 \quad \forall v \in P^k \left(I_{\alpha_i}^i \right), \quad \alpha_i = 1, \dots, N_i, \quad (3.12a)$$

$$\beta h^{-1} \left[\mathcal{P}^{(x^i)} w \right] + \left\{ \partial_{x^i} \left(\mathcal{P}^{(x^i)} w \right) \right\} \Big|_{x_{\alpha_i+1/2}^i} = w_{x^i} \Big|_{x_{\alpha_i+1/2}^i}, \quad (3.12b)$$

$$\left\{ \mathcal{P}^{(x^i)} w \right\} \Big|_{x_{\alpha_i+1/2}^i} = w \Big|_{x_{\alpha_i+1/2}^i}, \quad (3.12c)$$

where periodic extensions are used at the domain boundary.

Similarly to the one-dimensional case, there is an approximation result for the above multi-dimensional projection:

$$\|\mathcal{P}w - w\| \leq Ch^{k+1}|w|_{k+1}, \quad (3.13)$$

where C is independent of h .

Finally, we list some inverse properties of the finite element space W_h that will be used in our error analysis. For any function $w_h \in W_h$, the following inverse inequalities hold (Ciarlet, 1978):

$$\|\partial_x^l w_h\| \leq Ch^{-l}\|w_h\|, \quad (3.14a)$$

$$\|w_h\|_{\Gamma_h} \leq Ch^{-1/2}\|w_h\|, \quad (3.14b)$$

$$\|w_h\|_{\infty} \leq Ch^{-d/2}\|w_h\|, \quad (3.14c)$$

where d is the spatial dimension, and Γ_h denotes the boundary sets of all elements K_α .

3.4 Error estimates

Let us first present two technical lemmas, which will be used in the proof of the main result.

LEMMA 3.1 For $k \geq 1$ and $\eta \in W_h$, the linear functional $w \rightarrow A_i(\mathcal{P}w - w, \eta^*)$ is continuous on H^{k+2} with norm bounded by $C\|\eta\|$, where C is independent of h .

Proof. Let us use the notation $\int_{\Gamma_h} := \sum_{e \in \Gamma_h} \int_e$ and set $\xi := \mathcal{P}w - w$; we have

$$A(\xi, \eta^*) = \sum_{K \in \mathcal{T}_h} \int_K \nabla \xi \cdot \nabla \eta^* \, dx + \int_{\Gamma_h} (\widehat{\partial_n \xi} [\eta^*] + [\xi] \{\partial_n \eta^*\}) \, ds,$$

which can be written as

$$A(\xi, \eta^*) = \sum_{i=1}^d A_i(\xi, \eta^*),$$

where

$$A_i(\xi, \eta^*) = \sum_{\alpha=1}^N \left(\int_{K_\alpha} \xi_{x^i} \eta_{x^i}^* \, dx + \int_{K_\alpha / I_{\alpha_i}^1} (\widehat{\partial_{x^i} \xi} [\eta^*] + [\xi] \{\partial_{x^i} \eta^*\})_{x_{\alpha_i+1/2}^i} \, d\hat{x}^i \right)$$

with $d\hat{x}^i = \prod_{j \neq i} dx^j$. The proof of the approximation results for A_i , $i = 1, \dots, d$ are analogous; therefore, we present only the one for A_1 . Here we use an argument similar to the one in the proof of Cockburn *et al.* (2001, Lemma 3.6) for a local projection.

Using integration by parts we have

$$A_1(\xi, \eta^*) = - \sum_{\alpha} \left(\int_{K_\alpha} \xi \eta_{x^1 x^1}^* \, dx + \int_{K_\alpha / I_{\alpha_1}^1} (-\widehat{\xi_{x^1}} [\eta^*] + [\xi] [\eta_{x^1}^*])_{x_{\alpha_1+1/2}^1} \, d\hat{x}^1 \right);$$

then

$$\begin{aligned} |A_1(\xi, \eta^*)| &\leq \sum_{\alpha} \left| \int_{K_{\alpha}} \xi \eta_{x^1 x^1}^* dx + \int_{K_{\alpha}/I_{\alpha_1}^1} (-\widehat{\xi}_{x^1}[\eta^*] + \{\xi\}[\eta_{x^1}^*])_{x_{\alpha_1+1/2}^1} dx^1 \right| \\ &\leq \|\xi\| \|\eta_{x^1 x^1}\| + \sum_{\alpha} \int_{K_{\alpha}/I_{\alpha_1}^1} \left| (-\widehat{\xi}_{x^1}[\eta^*] + \{\xi\}[\eta_{x^1}^*])_{x_{\alpha_1+1/2}^1} \right| dx^1. \end{aligned} \quad (3.15)$$

Set $I = I_{\alpha_1}^1 \cup I_{\alpha_1+1}^1$; we use the trace inequality to obtain

$$\begin{aligned} \left| (-\widehat{\xi}_{x^1}[\eta^*])_{x_{\alpha_1+1/2}^1} \right| &\leq \|[\eta^*]\| \left(\frac{\beta}{h} \|[\xi]\| + \|\{\xi_{x^1}\}\| \right) \\ &\leq Ch^{-1/2} \|\eta\|_{0,I} (h^{-1-1/2} \|\xi\|_{0,I} + h^{-1/2} \|\xi_{x_1}\|_{0,I} + h^{1-1/2} \|\xi_{x_1 x_1}\|_{0,I}) \\ &\leq C \|\eta\|_{0,I} (h^{-2} \|\xi\|_{0,I} + h^{-1} \|\xi_{x_1}\|_{0,I} + \|\xi_{x_1 x_1}\|_{0,I}). \end{aligned}$$

Similarly,

$$\begin{aligned} \left| (\{\xi\}[\eta_{x^1}^*])_{x_{\alpha_1+1/2}^1} \right| &\leq Ch^{-1/2} \|\eta_{x^1}\|_{0,I} (h^{-1/2} \|\xi\|_{0,I} + h^{1/2} \|\xi_{x_1}\|_{0,I}) \\ &\leq Ch \|\eta_{x^1}\|_{0,I} (h^{-2} \|\xi\|_{0,I} + h^{-1} \|\xi_{x_1}\|_{0,I}). \end{aligned}$$

Substitution of these estimates into (3.15) yields

$$|A_1(\xi, \eta^*)| \leq C(\|\eta\| + h \|\eta_{x_1}\| + h^2 \|\eta_{x_1 x_1}\|) (h^{-2} \|\xi\| + h^{-1} \|\xi_{x_1}\| + \|\xi_{x_1 x_1}\|). \quad (3.16)$$

By Liu (2015, Corollary 7.2), we have for $m = 0, 1, 2$,

$$|\xi|_m^2 = \sum_{\alpha} \sum_{|\zeta|=m} \|\partial_x^{\zeta} (\mathcal{P}w - w)\|_{0, K_{\alpha}}^2 \leq Ch^{2(k+1-m)} |w|_{k+1}^2. \quad (3.17)$$

Putting (3.17) into (3.16) and using the inverse inequalities for η we obtain

$$|A_1(\xi, \eta^*)| \leq Ch^{k-1} |w|_{k+1} \|\eta\| \leq C \|w\|_{k+2} \|\eta\|. \quad (3.18)$$

The proof of Lemma 3.1 is complete. \square

LEMMA 3.2 Let A be defined in (3.3). For $\xi = \mathcal{P}w - w$ with $w \in H^{k+2}$ and $\eta \in W_h$ we have

$$|A(\xi, \eta^*) - A(\xi^*, \eta)| \leq Ch^{k+2} |w|_{k+2} \|\eta\|, \quad (3.19)$$

where the constant C is independent of h .

Proof. We first claim that

$$A_1(\xi, \eta^*) = 0 \quad \forall w|_{K_\alpha} \in P^{k+1}(K_\alpha), \quad \eta \in W_h. \quad (3.20)$$

To prove this claim, we fix $\eta^* \in W_h$. Since \mathcal{P} is a polynomial-preserving operator, (3.20) holds true for every $w \in W_h$. Therefore, we need to consider only the cases

$$w(x)|_{K_\alpha} = a_\alpha (x^j)^{k+1},$$

where the constant a_α may vary from element to element. Below we shall use the notation $w_i = w(x^i)$ to denote dependence only on variable x^i .

For $j = 1$, we integrate by parts and obtain

$$A_1(\xi, \eta^*) = - \sum_\alpha \left(\int_{K_\alpha} \xi \eta_{x^1 x^1}^* dx + \int_{K_\alpha / I_{\alpha_1}^1} \left(-\widehat{\partial_{x^1} \xi} [\eta^*] + \{\xi\} [\partial_{x^1} \eta^*] \right)_{x_{\alpha_1+1/2}^1} d\hat{x}^1 \right);$$

we have $\mathcal{P}w = P^{(x^1)}w_1$ and $\eta_{x^1 x^1}^*$ is a polynomial of degree at most $k - 2$ in x^1 and we obtain

$$\sum_\alpha \int_{K_\alpha} (\mathcal{P}w - w) \eta_{x^1 x^1}^* dx = \sum_\alpha \int_{K_\alpha} \left(\mathcal{P}^{(x^1)}w_1 - w_1 \right) \eta_{x^1 x^1}^* dx = 0.$$

In addition, we have

$$\{\mathcal{P}w\} = \{\mathcal{P}^{(x^1)}w_1\} = \{w\}, \quad \widehat{\partial_{x^1}(\mathcal{P}w)} = \widehat{\partial_{x^1} \mathcal{P}^{(x^1)}w_1} = \widehat{\partial_{x^1} w}.$$

Thus, $A_1(\xi, \eta^*) = 0$ for $w|_{K_\alpha} = a_\alpha (x^1)^{k+1}$.

In the case $j \neq 1$, due to the special form of ξ we have $\partial_{x^1} \xi = \partial_{x^1} (\mathcal{P}w - w) = 0$ and

$$\mathcal{P}w = \mathcal{P}^{(x^j)}w_j$$

on the interface $x^1 = x_{\alpha_1+1/2}^1$, where $\widehat{\partial_{x^1} \xi} = 0$ and $[\xi] = 0$ by a direct check. We thus conclude that $A_1(\xi, \eta^*) = 0$ for $w|_{K_\alpha} = a_\alpha (x^j)^{k+1}$. This completes the proof of (3.20).

Due to (3.20), $A_1(\xi, \eta^*)$ vanishes over P^s for any $0 \leq s \leq k + 1$ when restricted to each K_α . Note that for $w = w \chi_{K_\alpha}$, we have $\mathcal{P}w = (\mathcal{P}w) \chi_{K_\alpha}$, hence $\xi = \xi \chi_{K_\alpha}$, where χ_K is the usual indicator function of K . By applying the Bramble–Hilbert lemma combined with the standard scaling argument on the restriction to K_α , we obtain

$$A_i(\xi, \eta^*) \leq Ch^{k+2} |w|_{k+2, K_\alpha} \|\eta\|_{0, \tilde{K}_\alpha},$$

where \tilde{K}_α includes K_α and its immediate neighboring cells. In general, for $w \in H^{k+2}$, we have $w = w \sum \chi_{K_\alpha}$, hence $\xi = \xi \sum \chi_{K_\alpha}$. Therefore

$$\begin{aligned} A_i(\xi, \eta^*) &= \sum A_i(\xi \chi_{K_\alpha}, \eta^*) \leq Ch^{k+2} \sum |w|_{k+2, K_\alpha} \|\eta\|_{0, \tilde{K}_\alpha} \\ &\leq Ch^{k+2} \left[\sum_\alpha |w|_{k+2, K_\alpha}^2 \right]^{1/2} \left[\sum_\alpha \|\eta\|_{0, K_\alpha}^2 \right]^{1/2}. \end{aligned}$$

Applying this to all A_i , we proceed with

$$|A(\xi, \eta^*)| \leq Ch^{k+2} |w|_{k+2} \|\eta\|.$$

Hence we have proved Lemma 3.2. □

We are now ready to present the error estimate result in the following.

THEOREM 3.3 Let u_h be the solution to the semidiscrete DG scheme (3.2), (3.3), (3.4) with any β except for $k(k + \cos(k + 1 + 2j/N)\pi)/2$ with j running from 0 to $N_i - 1$ for each fixed $i = 1, \dots, d$, and u a smooth solution to (3.1). Then we have the error estimate

$$\|u_h(\cdot, t) - u(\cdot, t)\| \leq Ch^{k+1}, \quad 0 \leq t \leq T, \quad (3.21)$$

where C depends on $\|u\|_{k+2}$, $\|u_t\|_{k+1}$, $\|\Phi\|_\infty$, T linearly and the data given, but is independent of h .

REMARK 3.4 In the multi-dimensional case, the proof of Theorem 3.3 requires stronger smoothness assumptions on the exact solution than those in the one-dimensional case.

Proof. The choice of β in the case $\theta = \frac{1}{2}$ is explained in Remark 2.2. The scheme consistency implies that for the exact solution u ,

$$i \int_\Omega u_t v \, dx = A(u, v) + \int_\Omega \Phi u v \, dx, \quad (3.22)$$

which when subtracted from equation (3.2) yields the error equation

$$i \int_\Omega (u - u_h)_t v \, dx = A(u - u_h, v) + \int_\Omega \Phi(u - u_h) v \, dx. \quad (3.23)$$

Let $\mathcal{P}u \in W_h$ be the projection of u defined in (3.12), and set

$$\eta = \mathcal{P}u - u_h, \quad \xi = \mathcal{P}u - u, \quad (3.24)$$

so that $u - u_h = \eta - \xi$, with which the error equation is written as

$$i \int_\Omega \eta_t v \, dx = i \int_\Omega \xi_t v \, dx + A(\eta - \xi, v) + \int_\Omega \Phi(\eta - \xi) v \, dx.$$

We take $v = \eta^*$ to obtain

$$i \int_{\Omega} \eta_t \eta^* dx = i \int_{\Omega} \xi_t \eta^* dx + A(\eta - \xi, \eta^*) + \int_{\Omega} \Phi(\eta - \xi) \eta^* dx. \quad (3.25)$$

Since the numerical fluxes have been made so that

$$A(\eta, \eta^*) = A(\eta^*, \eta). \quad (3.26)$$

Hence

$$i \frac{d}{dt} \|\eta\|^2 = 2i \operatorname{Re} \left(\int_{\Omega} \xi_t \eta^* dx \right) - 2i \operatorname{Im} \left(\int_{\Omega} \Phi \xi \eta^* dx \right) + A(\xi, \eta^*) - A(\xi^*, \eta). \quad (3.27)$$

In the multi-dimensional case, $A(\xi, \eta^*)$ or $A(\xi^*, \eta)$ is not necessarily zero, but still controllable with the superconvergence result in Lemma 3.2.

Putting (3.19) into equality (3.27), we obtain

$$\frac{d}{dt} \|\eta\|^2 \leq 2(\|\xi_t\| + \|\Phi\|_{\infty} \|\xi\|) \|\eta\| + C|u|_{k+2} h^{k+2} \|\eta\|. \quad (3.28)$$

Hence

$$\begin{aligned} \frac{d}{dt} \|\eta\| &\leq \|\xi_t\| + \|\Phi\|_{\infty} \|\xi\| + C|u|_{k+2} h^{k+2} \\ &\leq Ch^{k+1} (1 + \|\Phi\|_{\infty} + |u|_{k+2} h), \end{aligned} \quad (3.29)$$

where we have used (3.13) so that $\|\xi_t\| + \|\xi\| \leq C(|u_t|_{k+1} + |u|_{k+1})h^{k+1}$. Hence integration of (3.29) gives

$$\|\eta(\cdot, t)\| \leq \|\eta(\cdot, 0)\| + C(1 + \|\Phi\|_{\infty} + |u|_{k+2} h)h^{k+1} \leq Ch^{k+1}, \quad (3.30)$$

where we have used

$$\|\eta(\cdot, 0)\| = \|\mathcal{P}u_0 - \Pi_0 u_0\| \leq \|\mathcal{P}u_0 - u_0\| + \|u_0 - \Pi_0 u_0\| \leq Ch^{k+1}. \quad (3.31)$$

Upon using the triangle inequality with (3.13) we obtain the desired error estimate (3.21). \square

4. Error estimates for unstructured meshes with penalty

In this section we still consider equation (3.1) posed on $\Omega = \Pi_{i=1}^d [0, L_i] \subset \mathbb{R}^d$ subject to both initial data $u(x, 0) = u_0(x)$ and periodic boundary conditions. Here we derive the optimal error estimates for the DG method with penalty using unstructured meshes. Let \mathcal{T}_h be a shape-regular triangulation of Ω

such that $\bar{\Omega} = \cup_{K \in \mathcal{T}_h} \bar{K}$. For any element $K \in \mathcal{T}_h$, we assume that

$$\frac{\text{diam}(K)}{\rho_K} \leq \gamma \quad \forall K \in \mathcal{T}_h,$$

where $\text{diam}(K)$ is the diameter of K , ρ_K denotes the diameter of the maximum ball included in K .

The method in its global form is

$$i \int_{\Omega} u_h v \, dx = A(u_h, v) + \int_{\Omega} \Phi u_h v \, dx, \quad (4.1)$$

where

$$A(u_h, v) = \sum_{K \in \mathcal{T}_h} \int_K \nabla u_h \cdot \nabla v \, dx + \sum_{e \in \Gamma_h} \int_e \left(\frac{\beta}{h_e} [u_h] [v] + \{\partial_n u_h\} [v] + [u_h] \{\partial_n v\} \right) \, ds, \quad (4.2)$$

where on boundary faces both $[\cdot]$ and $\{\cdot\}$ are evaluated using periodic boundary conditions, and h_e is defined as in (3.5). The initial data for the resulting ordinary differential equation (4.1) is chosen as defined in (3.6).

4.1 Boundedness and stability

We first discuss the boundedness and stability of the bilinear form $A(\cdot, \cdot)$. Following the study by Arnold *et al.* (2002), we define the DG norm for $v \in V = V_h + H^2(\Omega)$:

$$\|v\| = \sum_{K \in \mathcal{T}_h} |v|_{1,K}^2 + \sum_{K \in \mathcal{T}_h} h^2 |v|_{2,K}^2 + \sum_{e \in \Gamma_h} h_e^{-1} |[v]|_e^2. \quad (4.3)$$

It is easy to verify that

$$|A(w, v)| \leq \Lambda \|w\| \cdot \|v\| \quad \forall w, v \in V, \quad (4.4)$$

where Λ is called the continuous constant. We also denote

$$\|v\|_E^2 := \sum_{K \in \mathcal{T}_h} |v|_{1,K}^2 + \sum_{e \in \Gamma_h} h_e^{-1} |[v]|_e^2.$$

LEMMA 4.1 There exist $\Gamma > 0$ and $\alpha > 0$ such that if $\beta > \Gamma$, then

$$A(v, v^*) \geq \alpha \|v\|^2 \quad \forall v \in V_h, \quad (4.5)$$

where α is called the coercive constant of $A(\cdot, \cdot)$ on V_h .

Proof. A direct calculation gives

$$\begin{aligned}
A(v, v^*) &= \sum_{K \in \mathcal{T}_h} \int_K |\nabla v|^2 \, dx + \sum_{e \in \Gamma_h} \frac{\beta}{h_e} \int_e |[v]|^2 \, ds + 2 \sum_{e \in \Gamma_h} \operatorname{Re} \int_e (\{\partial_n v^*\}[v]) \, ds \\
&\geq \sum_{K \in \mathcal{T}_h} \int_K |\nabla v|^2 \, dx + \sum_{e \in \Gamma_h} \frac{\beta}{h_e} \int_e |[v]|^2 \, ds - \left(\sum_{e \in \Gamma_h} \int_e |\{\partial_n v\}|^2 \, ds \right)^{1/2} \left(\sum_{e \in \Gamma_h} \int_e |[v]|^2 \, ds \right)^{1/2} \\
&\geq \sum_{K \in \mathcal{T}_h} \int_K |\nabla v|^2 \, dx - \frac{\epsilon h_e}{2} \sum_{e \in \Gamma_h} \int_e |\{\partial_n v\}|^2 \, ds + \left(\beta - \frac{1}{2} \epsilon^{-1} \right) \sum_{e \in \Gamma_h} h_e^{-1} \int_e |[v]|^2 \, ds.
\end{aligned}$$

Set

$$\Gamma \geq \frac{1}{4} \sup_{v \in V_h} \frac{h_e \sum_{e \in \Gamma_h} \int_e |\{\partial_n v\}|^2 \, ds}{\sum_{K \in \mathcal{T}_h} \int_K |\nabla v|^2 \, dx}. \quad (4.6)$$

We have

$$A(v, v^*) \geq (1 - 2\epsilon\Gamma) \sum_{K \in \mathcal{T}_h} \int_K |\nabla v|^2 \, dx + \left(1 - \frac{1}{2\beta\epsilon}\right) \sum_{e \in \Gamma_h} \beta h_e^{-1} \int_e |[v]|^2 \, ds \geq \alpha_1 \|v\|_E^2,$$

where $\alpha_1 = (1 - 2\epsilon\Gamma) \min\{1, \beta\}$ with

$$1 - 2\epsilon\Gamma = 1 - \frac{1}{2\beta\epsilon} = 1 - \sqrt{\frac{\Gamma}{\beta}} > 0,$$

provided $\epsilon = \frac{1}{2}(\Gamma\beta)^{-1/2}$ and $\beta > \Gamma$. Finally, using inverse inequalities, we have

$$\alpha_1 \|v\|_E^2 \geq \alpha \|v\|_h^2, \quad v \in V_h.$$

This completes the proof. \square

REMARK 4.2 We remark that the right-hand side of (4.6) is a finite number due to scaling and the fact that V_h is a finite-dimensional space. In some cases we can derive a sharper bound on Γ . For example, for rectangular meshes satisfying

$$\min_i \frac{h^i}{h} \geq \sigma > 0,$$

we fix a cell $K = K_\alpha$ and recall the estimate for any $v \in P^m[(a, b)]$,

$$\max\{|v(a)|^2, |v(b)|^2\} \leq \frac{(m+1)^2}{b-a} \int_a^b v^2(x) \, dx,$$

which is obtained in the study by [Warburton & Hesthaven \(2003\)](#), so that we have

$$\begin{aligned} \int_{\partial K} |\partial_n v|^2 ds &= \sum_{i=1}^d \int_{K_\alpha / I_{\alpha_i}^i} |\partial_{x^i} v|_{x^i=x_{\alpha_i \pm 1/2}^i}^2 d\hat{x}^i \\ &\leq \sum_{i=1}^d \frac{2k^2}{h^i} \int_K |\partial_{x^i} v|^2 dx \\ &\leq \frac{2k^2}{h\sigma} \int_K |\nabla_x v|^2 dx, \end{aligned}$$

where $d\hat{x}^i = \prod_{j \neq i} dx^j$. Therefore, using $h_e = h^i \leq h$, we have

$$h_e \sum_{e \in \Gamma_h} \int_e |\{\partial_n v\}|^2 ds \leq \frac{h_e}{2} \sum_{K \in \mathcal{T}_h} \int_{\partial K} |\partial_n v|^2 ds \leq \frac{k^2}{\sigma} \sum_{K \in \mathcal{T}_h} \int_K |\nabla v|^2 dx.$$

This indicates that Γ can be taken as $\frac{k^2}{4\sigma}$; therefore it suffices to choose β such that $\beta > \frac{k^2}{4\sigma}$.

4.2 Projection and approximation properties

We first introduce a projection and then present the approximation properties. Define the projection Π of a function w into space V_h as

$$\int_{\Omega} (w - \Pi w)v dx + A(w - \Pi w, v) = 0 \quad \forall v \in V_h. \quad (4.7)$$

This projection is uniquely defined since for $w = 0$ with $v = -\Pi w$ we have

$$0 = \|v\|^2 + A(v, v) \geq \|v\|^2 + \alpha \|v\|^2 \quad \forall v \in V_h,$$

where we have used (4.5). Thus ensures uniqueness for $v \equiv 0$.

THEOREM 4.3 For $w \in H^{k+1}$ and h suitably small, we have the following projection error:

$$\|w - \Pi w\| \leq Ch^{k+1}|w|_{k+1} \quad \text{and} \quad \|w - \Pi w\| \leq Ch^k|w|_{k+1}, \quad (4.8)$$

where C depends on $k, d, 1/\alpha, \Lambda$ and the shape parameter γ of meshes.

Proof. We carry out the proof in two steps:

Step 1. We first bound the projection error $R := w - \Pi w$ in the following way: for any $v \in V_h$, we have

$$\begin{aligned} \alpha \|v - \Pi w\|^2 &\leq A(v - \Pi w, v - \Pi w) \\ &= A(v - w, v - \Pi w) + \int_{\Omega} (\Pi w - w)(v - \Pi w) dx \\ &\leq \Lambda \|v - w\| \cdot \|v - \Pi w\| + \|R\| \cdot \|v - \Pi w\|. \end{aligned}$$

By the triangle inequality we obtain

$$\begin{aligned} \|R\|^2 &\leq 2 \inf_{v \in V_h} (\|v - w\|^2 + \|v - \Pi w\|^2) \\ &\leq C \inf_{v \in V_h} (\|v - w\|^2 + \|v - w\| \cdot \|v - \Pi w\| + \|R\| \cdot \|v - \Pi w\|) \\ &\leq C(\|Qw - w\|^2 + \|Qw - w\| \cdot \|Qw - \Pi w\| + \|R\| \cdot \|Qw - \Pi w\|) \end{aligned}$$

for C denoting $2 \max\{1, \Lambda/\alpha, 1/\alpha\}$. Here we have taken $v = Qw \in V_h$ to be the usual interpolant polynomial such that

$$\|\partial_x^m(w - Qw)\|_K \leq Ch^{k+1-m}|w|_{k+1,K},$$

where C depends on k, d and γ (Ciarlet, 1978).

This, when combined with the estimate

$$|w|_{0,\partial K}^2 \leq C(h^{-1}|w|_{0,K}^2 + h|w|_{1,K}^2),$$

yields

$$\|w - Qw\|^2 \leq Ch^{2k}|w|_{k+1,\Omega}^2. \quad (4.9)$$

Therefore

$$\begin{aligned} \|R\|^2 &\leq C(h^{2k}|w|_{k+1}^2 + h^k|w|_{k+1}\|R\| + h^{k+1}|w|_{k+1}\|R\| + \|R\|^2) \\ &\leq (C + 1/2)h^{2k}|w|_{k+1}^2 + \frac{1}{2}\|R\|^2 + \frac{C}{2}h^{2k+2}|w|_{k+1}^2 + \frac{3C}{2}\|R\|^2. \end{aligned}$$

Hence

$$\|R\|^2 \leq (1 + 2C + Ch^2)h^{2k}|w|_{k+1}^2 + 3C\|R\|^2. \quad (4.10)$$

Step 2. We proceed to obtain $\|R\|$ by coupling with a duality argument. Define the auxiliary function ψ as the solution of the adjoint problem

$$\begin{cases} \psi - \Delta\psi = R & \text{in } \Omega, \\ \psi \text{ satisfies the periodic boundary condition on } \partial\Omega. \end{cases} \quad (4.11)$$

This problem has a unique solution and admits the following regularity estimate for $\psi \in H^2(\Omega)$:

$$\|\psi\|_2 \leq \|R\|. \quad (4.12)$$

We then have

$$\begin{aligned}
\|R\|^2 &= \sum_{K \in \mathcal{T}_h} \int_K R^*(\psi - \Delta\psi) \, dx \\
&= \sum_{K \in \mathcal{T}_h} \int_K R^* \psi \, dx + \sum_{K \in \mathcal{T}_h} \int_K \nabla R^* \cdot \nabla \psi \, dx + \sum_{K \in \mathcal{T}_h} \int_{\partial K} -R^* \frac{\partial \psi}{\partial n} \, ds \\
&= \sum_{K \in \mathcal{T}_h} \int_K R^* \psi \, dx + \sum_{K \in \mathcal{T}_h} \int_K \nabla R^* \cdot \nabla \psi \, dx \\
&\quad + \sum_{e \in \Gamma_h} \int_e \left(\frac{\beta}{h} \int_e [R^*][\psi] + \{\partial_n R^*\}[\psi] + [R^*]\{\partial_n \psi\} \right) \, ds \\
&= \int_{\Omega} R^* \psi \, dx + A(R^*, \psi) \\
&= \int_{\Omega} R \psi^* \, dx + A(R, \psi^*).
\end{aligned} \tag{4.13}$$

For $k \geq 1$, we take $\psi_h \in V_h$ to be a piecewise linear interpolant of ψ so that

$$\|\partial_x^m(\psi - \psi_h)\| \leq Ch^{2-m}|\psi|_2, \quad m = 0, 1, 2.$$

From (4.7) it follows that $\int_{\Omega} Rv \, dx + A(R, v) = 0$ for any $v \in V_h$. Using this formula with $v = \psi_h^*$ we obtain

$$\begin{aligned}
\|R\|^2 &= \int_{\Omega} R \psi^* \, dx + A(R, \psi^*) = \int_{\Omega} R(\psi^* - \psi_h^*) \, dx + A(R, \psi^* - \psi_h^*) \\
&\leq \|R\| \cdot \|\psi - \psi_h\| + A\|R\| \cdot \|\psi - \psi_h\| \\
&\leq Ch^2|\psi|_2\|R\| + Ch|\psi|_2\|R\| \\
&\leq C(h^2\|R\| + h\|R\|)\|R\|,
\end{aligned} \tag{4.14}$$

where we have used (4.12). Hence

$$\|R\| \leq Ch(h\|R\| + \|R\|). \tag{4.15}$$

For $h \leq 1/\sqrt{2C}$, (4.15) yields

$$\|R\| \leq \frac{Ch}{1 - Ch^2} \|R\| \leq 2Ch\|R\|.$$

This upon substitution into (4.10) gives

$$(1 - 12C^3h^2)\|R\|^2 \leq (1 + 2C + Ch^2)h^{2k}|w|_{k+1}^2.$$

Further taking $h^2 \leq \frac{1}{24C^3}$ we have

$$\|R\|^2 \leq (3 + 4C)h^{2k}|w|_{k+1}^2.$$

Hence for h suitably small,

$$\|R\| \leq Ch^{k+1}|w|_{k+1} \quad \text{and} \quad \|R\| \leq Ch^k|w|_{k+1}.$$

The proof is now complete. \square

4.3 *A priori error estimate*

We are left to carry out the error analysis for the DG method by using the projection result (4.8). The consistency of the DG method requires that the exact solution u satisfies

$$i \int_{\Omega} u_t v \, dx = A(u, v) + \int_{\Omega} \Phi u v \, dx \quad \forall v \in V_h. \quad (4.16)$$

Hence we have the error equation

$$i \int_{\Omega} (u_t - u_{ht}) v \, dx = A(u - u_h, v) + \int_{\Omega} \Phi(u - u_h) v \, dx \quad \forall v \in V_h. \quad (4.17)$$

Set $\xi = \Pi u - u$, $\eta = \Pi u - u_h$; we get

$$i \int_{\Omega} \eta_t v \, dx = i \int_{\Omega} \xi_t v \, dx + A(\eta, v) - A(\xi, v) + \int_{\Omega} \Phi(\eta - \xi) v \, dx. \quad (4.18)$$

Take $v = \eta^*$; we have

$$i \int_{\Omega} \eta_t \eta^* \, dx = i \int_{\Omega} \xi_t \eta^* \, dx + A(\eta, \eta^*) - A(\xi, \eta^*) + \int_{\Omega} \Phi(\eta - \xi) \eta^* \, dx. \quad (4.19)$$

Thus

$$\frac{d}{dt} \|\eta\|^2 = 2 \operatorname{Re} \left(\int_{\Omega} \xi_t \eta^* \, dx \right) - 2 \operatorname{Im} (A(\xi, \eta^*)) - 2 \operatorname{Im} \left(\int_{\Omega} \Phi \xi \eta^* \, dx \right). \quad (4.20)$$

Note that $A(\xi, \eta^*) = - \int_{\Omega} \xi \eta^* \, dx$; we thus have

$$\begin{aligned} \frac{d}{dt} \|\eta\|^2 &\leq 2 \|\xi_t\| \cdot \|\eta\| + 2 \|\xi\| \cdot \|\eta\| + 2 \|\Phi\|_{\infty} \|\xi\| \cdot \|\eta\| \\ &\leq (2 \|\xi_t\| + 2 \|\xi\| + 2 \|\Phi\|_{\infty} \|\xi\|) \|\eta\| \\ &\leq Ch^{k+1} \|\eta\|, \end{aligned} \quad (4.21)$$

where C depends on $|u|_{k+1}$, $|u_t|_{k+1}$ and $\|\Phi\|_\infty$. A direct integration gives

$$\|\eta(\cdot, t)\| \leq \|\eta(\cdot, 0)\| + CTh^{k+1} \leq C(1 + T)h^{k+1}, \quad t \leq T. \quad (4.22)$$

Here we have used the fact $\|\eta(\cdot, 0)\| = \|\Pi u_0 - \Pi_0 u_0\| \leq Ch^{k+1}$. The L^2 optimal error estimate is thus verified.

The main result can now be summarized as follows.

THEOREM 4.4 Let u_h be the solution to the semidiscrete DG scheme (4.1), (4.2) with $\beta > \Gamma$, which depends on the degree k of the polynomial elements, and u be the smooth solution of (3.1). Then we have the error estimate

$$\|u(\cdot, t) - u_h(\cdot, t)\| \leq Ch^{k+1}, \quad 0 \leq t \leq T,$$

where C depends on $|u|_{k+1}$, $|u_t|_{k+1}$, $\|\Phi\|_\infty$, T linearly, β and $\|u_0\|_{k+1}$, but is independent of h .

REMARK 4.5 The analysis above and accuracy results can be generalized to the case with other boundary conditions. For example, for the Dirichlet boundary condition with $u(x, t) = g$ for $x \in \partial\Omega$, the corresponding DG scheme becomes

$$i \int_{\Omega} u_h v \, dx = A(u_h, v) + \int_{\Omega} \Phi(x) u_h v \, dx + L(v),$$

where

$$\begin{aligned} A(u_h, v) &= \sum_{K \in \mathcal{T}_h} \int_K \nabla u_h \cdot \nabla v \, dx \\ &\quad + \sum_{e \in \Gamma_h^0} \int_e \left((\beta h_e^{-1} [u_h] + \{\partial_n u_h\}) [v] + [u_h] \{\partial_n v\} \right) \, ds \\ &\quad - \sum_{e \in \Gamma_h^\partial} \int_e \left((\beta h_e^{-1} (0 - u_h) + \partial_n u_h) v + (u_h - 0) \partial_n v \right) \, ds, \\ L(v) &= - \sum_{e \in \Gamma_h^\partial} \int_e (\beta h_e^{-1} g v - g \partial_n v) \, ds. \end{aligned}$$

Here the boundary condition is weakly enforced in such a way that the boundary data are used whenever available, otherwise the trace of the numerical solution in corresponding boundary faces will be used. Our numerical tests (see Example 5.4) on the case with Dirichlet boundary data indeed show similar convergence behavior to the examples with periodic boundary conditions.

5. Numerical examples

In this section, we present numerical examples to verify our theoretical findings, based on the MPDG formulation (3.2) with (3.4). In order to preserve mass at the fully discrete level, we follow Lu *et al.* (2015) to adopt the Crank–Nicolson method in the time discretization for linear Schrödinger equations,

and the Strang splitting method for nonlinear Schrödinger equations. Both methods are second order in time.

Here numerical examples are mainly in a two-dimensional setting, and we refer to the study by Lu *et al.* (2015) for extensive one-dimensional numerical examples.

The L^2 errors are defined by

$$\|u^R - u_h^R\| := \left(\int_{\Omega} (u^R(\cdot, T) - u_h^R(\cdot, T))^2 dx \right)^{1/2}, \quad \|u^I - u_h^I\| := \left(\int_{\Omega} (u^I(\cdot, T) - u_h^I(\cdot, T))^2 dx \right)^{1/2},$$

where u^R and u^I denote the real part and imaginary parts of u , respectively.

EXAMPLE 5.1 We consider the $(2\pi, 2\pi)$ -periodic initial value problem for the two-dimensional linear Schrödinger equation

$$iu_t + \Delta u - \Phi(x, y)u = f(x, y, t), \quad 0 < x, y < 2\pi, \quad 0 < t \leq T,$$

where the potential $\Phi(x, y) = \sin(x + y)$, and $f(x, y, t) = -(1 + \sin(x + y))e^{i(x+y-t)}$. The exact solution to this problem is

$$u(x, y, t) = e^{i(x+y-t)}.$$

We test this example using the P^k polynomials with $k = 1, 2, 3, 4$ on a uniform mesh with $N \times N$ cells of equal mesh sizes, $h_x = h_y = \frac{2\pi}{N}$. The second-order Crank–Nicolson time discretization with $\Delta t \sim h^{\lceil \frac{k+1}{2} \rceil}$ is used so that the error from the spatial discretization dominates. Our numerical experiments show that the optimal order of accuracy can be achieved for P^k , $k = 1, 3, 4$ approximations with different β and θ . In Table 1, we report the L^2 errors and orders of accuracy for P^k , $k = 1, 3, 4$ polynomials with only $\beta = 0$ and $\theta = \frac{1}{2}$. For the P^2 approximation, the convergence rate in terms of L^2 errors appears to rely on the choice of β when $\theta = \frac{1}{2}$. Table 2 shows that the order of accuracy for P^2 polynomials is oscillating for $(\beta, \theta) = (0, \frac{1}{2})$, but the optimal order of accuracy is achieved by taking suitably large β such as $(\beta, \theta) = (15, \frac{1}{2})$. Alternatively, the optimal third order of accuracy can also be achieved for $\beta = 0$ if $\theta = 1$.

EXAMPLE 5.2 We consider the linear Schrödinger equation

$$iu_t + \Delta u = 0, \quad u(x, y, 0) = e^{-i(x+y)}, \quad (x, y) \in [0, 2\pi]^2, \quad t > 0,$$

with periodic boundary condition. The exact solution to this problem is

$$u(x, y, t) = e^{-i(x+y+2t)}.$$

We test this example using P^k polynomials with $k = 1, 2$ on a uniform mesh with $N \times N$ cells. The flux parameter is taken as $\beta = 10$. For the P^1 and P^2 approximations, we take $(N, \Delta t) = (80, 0.005)$ and $(N, \Delta t) = (40, 0.002)$, respectively. The time histories of errors and mass are shown in Fig. 1. Here the L^2 error is defined by

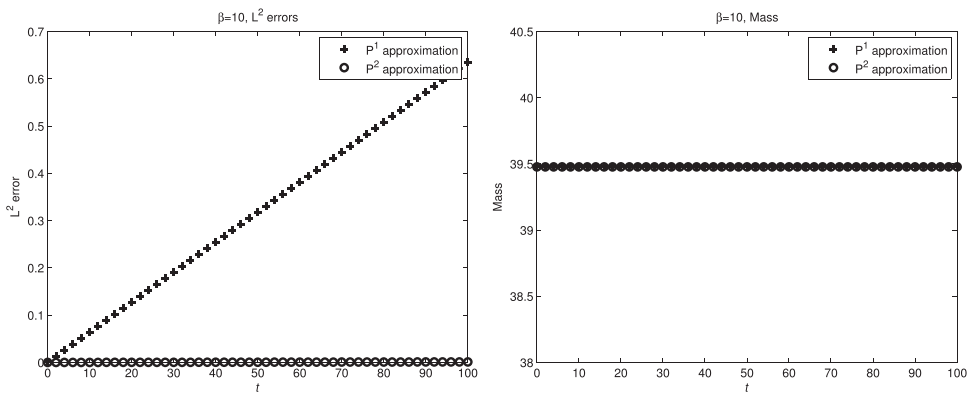
$$\|u(\cdot, t) - u_h(\cdot, t)\|_{L^2} = \left(\|u^R(\cdot, t) - u_h^R(\cdot, t)\|_{L^2}^2 + \|u^I(\cdot, t) - u_h^I(\cdot, t)\|_{L^2}^2 \right)^{1/2}.$$

TABLE 1 Errors for Example 5.1 when using P^k , $k = 1, 3, 4$ polynomials on a uniform mesh of $N \times N$ cells, $\theta = \frac{1}{2}$. Final time is $T = 1$

$k = 1$	Δt	N	$2.0 \cdot 10^{-2}$	$1.0 \cdot 10^{-2}$	$5.0 \cdot 10^{-3}$	$2.5 \cdot 10^{-3}$	Δt	N	$2.0 \cdot 10^{-2}$	$1.0 \cdot 10^{-2}$	$5.0 \cdot 10^{-3}$	$2.5 \cdot 10^{-3}$
$\beta = 0$	$\ u^R - u_h^R\ $	$3.45 \cdot 10^{-1}$	$7.96 \cdot 10^{-2}$	$1.92 \cdot 10^{-2}$	$4.77 \cdot 10^{-3}$	$1.20 \cdot 10^{-3}$	$\ u' - u_h'\ $	$3.14 \cdot 10^{-1}$	$7.31 \cdot 10^{-2}$	$1.76 \cdot 10^{-2}$	$4.39 \cdot 10^{-3}$	$2.00 \cdot 10^{-3}$
	Order	—	2.12	2.05	2.01	—	Order	—	2.10	2.05	2.05	2.00
$k = 3$	Δt	N	$2.0 \cdot 10^{-2}$	$5.0 \cdot 10^{-3}$	$1.25 \cdot 10^{-3}$	$3.125 \cdot 10^{-4}$	Δt	N	$2.0 \cdot 10^{-2}$	$5.0 \cdot 10^{-3}$	$1.25 \cdot 10^{-3}$	$3.125 \cdot 10^{-4}$
	Order	—	10	20	40	80	Order	—	10	20	40	80
$\beta = 0$	$\ u^R - u_h^R\ $	$4.61 \cdot 10^{-4}$	$3.96 \cdot 10^{-5}$	$2.47 \cdot 10^{-6}$	$1.03 \cdot 10^{-7}$	$4.58 \cdot 10^{-8}$	$\ u' - u_h'\ $	$4.78 \cdot 10^{-4}$	$4.04 \cdot 10^{-5}$	$2.52 \cdot 10^{-6}$	$1.08 \cdot 10^{-7}$	$4.54 \cdot 10^{-8}$
	Order	—	3.54	4.00	4.00	—	Order	—	3.56	4.00	—	4.54
$k = 4$	Δt	N	$2.0 \cdot 10^{-2}$	$2.5 \cdot 10^{-3}$	$3.125 \cdot 10^{-4}$	—	Δt	N	$2.0 \cdot 10^{-2}$	$2.5 \cdot 10^{-3}$	$3.125 \cdot 10^{-4}$	—
	Order	—	10	20	40	—	Order	—	10	20	40	—
$\beta = 0$	$\ u^R - u_h^R\ $	$3.48 \cdot 10^{-4}$	$5.46 \cdot 10^{-6}$	$9.21 \cdot 10^{-8}$	—	$\ u' - u_h'\ $	$3.71 \cdot 10^{-4}$	$5.81 \cdot 10^{-6}$	$9.72 \cdot 10^{-8}$	—	—	—
	Order	—	5.99	5.89	—	—	Order	—	6.00	5.90	—	—

TABLE 2 Errors for Example 5.1 when using P^2 polynomials on a uniform mesh of $N \times N$ cells. Final time is $T = 1$

$\theta = \frac{1}{2}$	Δt	2.0 e^{-02}	5.00 e^{-03}	1.25 e^{-03}	3.125 e^{-04}	Δt	2.0 e^{-02}	5.00 e^{-03}	1.25 e^{-03}	3.125 e^{-04}
	N	10	20	40	80	N	10	20	40	80
$\beta = 0$	$\ u_h^R - u_h^R\ $	1.66 e^{-02}	1.20 e^{-03}	1.28 e^{-03}	9.87 e^{-05}	$\ u_h^I - u_h^I\ $	1.71 e^{-02}	1.11 e^{-03}	1.28 e^{-03}	1.03 e^{-04}
	order	—	3.79	-0.09	3.70	order	—	3.95	-0.21	3.64
$\beta = 15$	$\ u_h^R - u_h^R\ $	1.07 e^{-02}	1.33 e^{-03}	1.65 e^{-04}	1.14 e^{-05}	$\ u_h^I - u_h^I\ $	1.07 e^{-02}	1.33 e^{-03}	1.65 e^{-04}	1.14 e^{-05}
	order	—	3.01	3.01	3.86	order	—	3.01	3.01	3.86
$\theta = 1$	Δt	2.0 e^{-02}	5.00 e^{-03}	1.25 e^{-03}	3.125 e^{-04}	Δt	2.0 e^{-02}	5.00 e^{-03}	1.25 e^{-03}	3.125 e^{-04}
	N	10	20	40	80	N	10	20	40	80
$\beta = 0$	$\ u_h^R - u_h^R\ $	1.00 e^{-02}	4.61 e^{-03}	5.83 e^{-04}	5.86 e^{-05}	$\ u_h^I - u_h^I\ $	9.18 e^{-03}	4.47 e^{-03}	5.64 e^{-04}	5.92 e^{-05}
	order	—	1.12	2.98	3.31	order	—	1.04	2.99	3.25

FIG. 1. L^2 errors and mass history with $\beta = 10$, P^k , $k = 1, 2$ approximation.

It shows that the L^2 error of the P^2 approximation is much smaller than that of the P^1 approximation, and the scheme preserves the mass as expected.

EXAMPLE 5.3 We consider the two-dimensional linear Schrödinger equation

$$\begin{aligned} iu_t + \Delta u + \Phi(x, y)u = 0, \quad (x, y) \in \Omega = [-20, 20] \times [-20, 20], \quad 0 < t < 1, \\ u(x, y, 0) = \frac{i}{2 \cosh x \cosh y}, \end{aligned}$$

subject to the Dirichlet boundary condition $u(x, y, t) = g$ on the domain boundary $\partial\Omega$. Consider the potential

$$\Phi(x, y) = 3 - 2 \tanh^2 x - 2 \tanh^2 y,$$

and appropriate g so that the exact solution becomes a plane wave solution

$$u(x, y, t) = \frac{ie^{it}}{2 \cosh x \cosh y}.$$

Here g is taken as the trace of u .

We test this example using P^k polynomials with $k = 1, 2$ in the DG scheme given in Remark 4.5, on a uniform mesh of $N \times N$ cells. Again the Crank–Nicolson time discretization is used. The results in Table 3 show that the order of convergence of the L^2 error achieves the expected $(k + 1)$ th order of accuracy. We have also observed the oscillation in errors for the P^2 approximation with $\theta = \frac{1}{2}$, and $\beta = 0$, yet the optimal third order of accuracy can be achieved for larger β . These are similar to the results for the DG method with a periodic boundary condition.

EXAMPLE 5.4 We consider the two-dimensional nonlinear Schrödinger equation

$$iu_t + \Delta u + 2|u|^2 u = 0,$$

TABLE 3 Errors for Example 5.3 when using P^k polynomials on a uniform mesh of $N \times N$ cells and $\theta = \frac{1}{2}$. Final time is $T = 1$

$k = 1$	Δt	1.0 e-01	5.0 e-02	2.5 e-02	Δt	1.0 e-01	5.0 e-02	2.5 e-02
	N	80	160	320	N	80	160	320
$\beta = 0$	$\ u^R - u_h^R\ $ order	4.30 e-02 —	7.76 e-03 2.47	1.82 e-03 2.09	$\ u^I - u_h^I\ $ order	3.82 e-02 —	6.76 e-03 2.50	1.52 e-03 2.15
$k = 2$	Δt	1.0 e-01	2.5 e-02	6.25 e-03	Δt	1.0 e-01	2.5 e-02	6.25 e-03
	N	80	160	320	N	80	160	320
$\beta = 0$	$\ u^R - u_h^R\ $ order	3.13 e-03 —	7.12 e-04 2.14	9.69 e-05 2.88	$\ u^I - u_h^I\ $ order	3.47 e-03 —	6.44 e-04 2.43	8.62 e-05 2.90
$k = 2$	Δt	1.0 e-01	2.5 e-02	6.25 e-03	Δt	1.0 e-01	2.5 e-02	6.25 e-03
	N	80	160	320	N	80	160	320
$\beta = 15$	$\ u^R - u_h^R\ $ order	9.28 e-04 —	8.20 e-05 3.50	1.21 e-05 2.76	$\ u^I - u_h^I\ $ order	1.16 e-03 —	1.15 e-04 3.33	1.71 e-05 2.75
$k = 2$	Δt	1.0 e-01	2.5 e-02	6.25 e-03	Δt	1.0 e-01	2.5 e-02	6.25 e-03
	N	80	160	320	N	80	160	320
$\beta = 20$	$\ u^R - u_h^R\ $ order	9.69 e-04 —	8.37 e-05 3.53	1.01 e-05 3.05	$\ u^I - u_h^I\ $ order	1.19 e-03 —	9.40 e-05 3.66	8.23 e-06 3.51

over the domain $[0, 2\pi]^2$, subject to initial condition

$$u(x, y, 0) = \sqrt{2}e^{i(x+y)},$$

and a periodic boundary condition. The exact solution is a plane wave solution

$$u(x, y, t) = \sqrt{2}e^{i(x+y+2t)}.$$

We test this example using P^k polynomials with $k = 1, 2, 3, 4$ with different θ and β , on a uniform mesh of $N \times N$ cells. The convergence results are similar to those for linear equations. In Tables 4–5, we list the L^2 errors and order of accuracy of P^k approximations, respectively. We see that the optimal $k + 1$ order of accuracy is achieved for P^k , $k = 1, 3, 4$ polynomials with $\beta = 0$, while for the P^2 approximation, the order of accuracy appears oscillating for $\beta = 0$ with $\theta = \frac{1}{2}$, and again we can obtain the optimal order of accuracy by taking $(\beta, \theta) = (10, \frac{1}{2})$ or $(\beta, \theta) = (0, 1)$.

6. Concluding remarks

In this paper, optimal L^2 error estimates for mass-preserving DG methods applied to multi-dimensional linear Schrödinger equations are proved. Our analysis is carried out for both uniform Cartesian meshes using tensor-product polynomial spaces, and arbitrary shape-regular meshes using regular polynomial spaces, and is valid for arbitrary polynomial degrees. The main ingredients in the proof are the

TABLE 4 Errors for Example 5.4 when using P^k , $k = 1, 3, 4$ polynomials on a uniform mesh of $N \times N$ cells and $\theta = \frac{1}{2}$. Final time is $T = 1$

$k = 1$	Δt	N	$2.0 \cdot 10^{-2}$	$1.0 \cdot 10^{-2}$	$5.0 \cdot 10^{-3}$	$2.5 \cdot 10^{-3}$	Δt	N	$2.0 \cdot 10^{-2}$	$1.0 \cdot 10^{-2}$	$5.0 \cdot 10^{-3}$	$2.5 \cdot 10^{-3}$
$\beta = 0$	order	$\ u^R - u_h^R\ $	$4.64 \cdot 10^{-1}$	$1.14 \cdot 10^{-1}$	$2.73 \cdot 10^{-2}$	$6.76 \cdot 10^{-3}$	$\ u^I - u_h^I\ $	$4.64 \cdot 10^{-1}$	$1.14 \cdot 10^{-1}$	$2.73 \cdot 10^{-2}$	$6.76 \cdot 10^{-3}$	40
		order	—	$2.0 \cdot 10^{-3}$	$2.0 \cdot 10^{-2}$	$2.0 \cdot 10^{-2}$	order	—	$2.0 \cdot 10^{-3}$	$2.0 \cdot 10^{-2}$	$2.0 \cdot 10^{-2}$	$2.0 \cdot 10^{-2}$
$k = 3$	Δt	N	$2.0 \cdot 10^{-2}$	$5.0 \cdot 10^{-3}$	$1.25 \cdot 10^{-3}$	$3.125 \cdot 10^{-4}$	Δt	N	$2.0 \cdot 10^{-2}$	$5.0 \cdot 10^{-3}$	$1.25 \cdot 10^{-3}$	$3.125 \cdot 10^{-4}$
		order	—	$1.0 \cdot 10^{-3}$	$3.94 \cdot 10^{-4}$	$1.13 \cdot 10^{-4}$	order	—	$1.0 \cdot 10^{-3}$	$3.94 \cdot 10^{-4}$	$1.13 \cdot 10^{-4}$	$3.94 \cdot 10^{-4}$
$\beta = 0$	order	$\ u^R - u_h^R\ $	$1.73 \cdot 10^{-3}$	$1.13 \cdot 10^{-4}$	$6.87 \cdot 10^{-6}$	$4.38 \cdot 10^{-7}$	$\ u^I - u_h^I\ $	$1.73 \cdot 10^{-3}$	$1.13 \cdot 10^{-4}$	$6.87 \cdot 10^{-6}$	$4.38 \cdot 10^{-7}$	80
		order	—	$1.0 \cdot 10^{-3}$	$3.97 \cdot 10^{-4}$	$3.125 \cdot 10^{-4}$	order	—	$1.0 \cdot 10^{-3}$	$3.97 \cdot 10^{-4}$	$3.125 \cdot 10^{-4}$	$3.97 \cdot 10^{-4}$
$k = 4$	Δt	N	$2.0 \cdot 10^{-2}$	$2.5 \cdot 10^{-3}$	$2.5 \cdot 10^{-3}$	$3.125 \cdot 10^{-4}$	Δt	N	$2.0 \cdot 10^{-2}$	$2.5 \cdot 10^{-3}$	$3.125 \cdot 10^{-4}$	$3.125 \cdot 10^{-4}$
		order	—	$1.0 \cdot 10^{-3}$	$3.99 \cdot 10^{-4}$	$4.12 \cdot 10^{-7}$	order	—	$1.0 \cdot 10^{-3}$	$3.99 \cdot 10^{-4}$	$4.12 \cdot 10^{-7}$	$3.99 \cdot 10^{-4}$
$\beta = 0$	order	$\ u^R - u_h^R\ $	$1.68 \cdot 10^{-3}$	$2.62 \cdot 10^{-5}$	$4.12 \cdot 10^{-7}$	$—$	$\ u^I - u_h^I\ $	$1.68 \cdot 10^{-3}$	$2.62 \cdot 10^{-5}$	$4.12 \cdot 10^{-7}$	$—$	5.99
		order	—	$6.00 \cdot 10^{-4}$	$5.99 \cdot 10^{-4}$	$—$	order	—	$6.00 \cdot 10^{-4}$	$5.99 \cdot 10^{-4}$	$—$	5.99

TABLE 5 Errors for Example 5.4 when using P^2 polynomials on a uniform mesh of $N \times N$ cells. Final time is $T = 1$

$\theta = \frac{1}{2}$	Δt	2.0 e^{-02}	5.0 e^{-03}	1.25 e^{-03}	3.125 e^{-04}	Δt	2.0 e^{-02}	5.0 e^{-03}	1.25 e^{-03}	3.125 e^{-04}
	N	10	20	40	80	N	10	20	40	80
$\beta = 0$	$\ u_h^R - u_h^R\ $	7.68 e^{-02}	8.45 e^{-03}	9.71 e^{-04}	2.36 e^{-04}	$\ u_h^I - u_h^I\ $	7.68 e^{-02}	8.45 e^{-03}	9.71 e^{-04}	2.36 e^{-04}
	order	—	3.18	3.12	2.04	order	—	3.18	3.12	2.04
$\beta = 10$	$\ u_h^R - u_h^R\ $	8.16 e^{-03}	1.22 e^{-03}	1.74 e^{-04}	2.11 e^{-05}	$\ u_h^I - u_h^I\ $	8.16 e^{-03}	1.22 e^{-03}	1.74 e^{-04}	2.11 e^{-05}
	order	—	2.74	2.81	3.04	order	—	2.74	2.81	3.04
$\theta = 1$	Δt	2.0 e^{-02}	5.0 e^{-03}	1.25 e^{-03}	3.125 e^{-04}	Δt	2.0 e^{-02}	5.0 e^{-03}	1.25 e^{-03}	3.125 e^{-04}
	N	10	20	40	80	N	10	20	40	80
$\beta = 0$	$\ u_h^R - u_h^R\ $	2.52 e^{-02}	5.53 e^{-03}	6.28 e^{-04}	3.25 e^{-05}	$\ u_h^I - u_h^I\ $	2.52 e^{-02}	5.53 e^{-03}	6.28 e^{-04}	3.25 e^{-05}
	order	—	2.19	3.14	4.27	order	—	2.19	3.14	4.27

construction and analysis of explicit global projections for the former setting, and implicit global projections for the latter setting if the flux parameter is suitably large. We also give numerical examples to verify the results of our theoretical analysis. We observe that the scheme for polynomials of even degree ($k = 2, 4$) shows peculiar convergence behavior when using the central numerical flux $\theta = \frac{1}{2}$, i.e., oscillation in L^2 errors for $k = 2$, and superconvergence for $k = 4$. For P^2 polynomials the optimal order of accuracy can be achieved by either using larger β if $\theta = \frac{1}{2}$, or using biased fluxes $\theta \neq \frac{1}{2}$ with $\beta = 0$. Such peculiar convergence behavior has also been observed for hyperbolic wave equations (see, e.g., Meng *et al.* 2016; Yi & Liu 2018) for odd-degree polynomials. Extension of this work to superconvergence results particularly for even-degree polynomials is interesting, and constitutes our future work.

Funding

National Science Foundation (DMS-1312636) and National Science Foundation Research Network (RNMS11-07291(KI-Net)) to H.L. National Natural Science Foundation of China (NSFC) Project (91430213) to Y.H. Hunan Provincial National Science Foundation Project (2016JJ6042) and National Natural Science Foundation of China (NSFC) Tian Yuan Fund (11626098) to W. L. NSFC Project (11671341), Hunan Provincial National Science Foundation Project (2015JJ2145) and Hunan Education Department Project (16A206) to N.Y.

Acknowledgements

We thank the referees for their valuable comments which led to significant improvements in this work.

REFERENCES

ARNOLD, D. N., BREZZI, F., COCKBURN, B. & MARINI, L. D. (2002) Unified analysis of discontinuous Galerkin methods for elliptic problems. *SIAM J. Numer. Anal.*, **39**, 1749–1779.

BAO, W. Z., JIN, S. & MARKOWICH, P. A. (2002) On time-splitting spectral approximations for the Schrödinger equation in the semiclassical regime. *J. Comput. Phys.*, **175**, 487–524.

BAUMANN, C. E. & ODEN, J. T. (1999) A discontinuous hp finite element method for convection–diffusion problems. *Comput. Methods Appl. Mech. Eng.*, **175**, 311–341.

BECERRIL, R., GUZMAN, F. S., RENDÓN–ROMERO, A. & VALDEZ–ALVARADO, S. (2008) Solving the time-dependent Schrödinger equation using finite difference methods. *Rev. Mex. Fís. E*, **54**, 120–132.

BONA, J., CHEN, H., KARAKASHIAN, O. & XING, Y. (2013) Conservative, discontinuous Galerkin–methods for the generalized Korteweg–de Vries equation. *Math. Comput.*, **82**, 1401–1432.

CASTILLO, P. (2000) An optimal error estimate for the local discontinuous Galerkin method. *Discontinuous Galerkin Methods: Theory, Computation and Applications* (B. Cockburn, G. Karniadakis & C.-W. Shu eds). Lecture Notes in Computational Science and Engineering, vol. 11, Berlin: Springer, pp. 285–290.

CASTILLO, P., COCKBURN, B., PERUGIA, I. & SCHÖTZAU, D. (2000) An *a priori* error analysis of the local discontinuous Galerkin method for elliptic problems. *SIAM J. Numer. Anal.*, **38**, 1676–1706.

CASTILLO, P., COCKBURN, B., SCHÖTZAU, D. & SCHWAB, C. (2002) Optimal *a priori* error estimates for the hp -version of the LDG method for convection–diffusion problems. *Math. Comput.*, **71**, 455–478.

CHANG, Q. S., JIA, E. H. & SUN, W. (1999) Difference schemes for solving the generalized nonlinear Schrödinger equation. *J. Comput. Phys.*, **148**, 397–415.

CHANG, Q. S. & WANG, G. B. (1990) Multigrid and adaptive algorithm for solving the nonlinear Schrödinger equation. *J. Comput. Phys.*, **88**, 362–380.

CHANG, Q. S. & XU, L. (1986) A numerical method for a system of generalized nonlinear Schrödinger equations. *J. Comput. Math.*, **4**, 191–199.

Ciarlet, P. G. (1978) *The Finite Element Method for Elliptic Problems*. Studies in Mathematics and its Applications, vol. 4. Amsterdam: North-Holland.

COCKBURN, B., KANSCHAT, G., PERUGIA, I. & SCHOTZAU, D. (2001) Superconvergence of the local discontinuous Galerkin method for elliptic problems on Cartesian grids. *SIAM J. Numer. Anal.*, **39**, 264–285.

COCKBURN, B. & SHU, C.-W. (1998) The local discontinuous Galerkin method for time-dependent convection–diffusion systems. *SIAM J. Numer. Anal.*, **35**, 2440–2463.

DELFOUR, M., FORTIN, M. & PAYR, G. (1981) Finite-difference solutions of a non-linear Schrödinger equation. *J. Comput. Phys.*, **44**, 277–288.

FEIT, M. D. & FLECK, J. A. (1983) Solution of the Schrödinger equation by a spectral method II: vibrational energy levels of triatomic molecules. *J. Chem. Phys.*, **78**, 301–308.

FEIT, M. D., FLECK, J. A. & STEIGER, A. (1982) Solution of the Schrödinger equation by a spectral method. *J. Comput. Phys.*, **47**, 412–433.

GRADINARU, V. (2007) Strang splitting for the time-dependent Schrödinger equation on sparse grids. *SIAM J. Numer. Anal.*, **46**, 103–123.

HERMANN, M. R. & FLECK, J. A. (1988) Split-operator spectral method for solving the time-dependent Schrödinger equation in spherical coordinates. *Phys. Rev. A*, **38**, 6000–6012.

JENSEN, A. (1986) Commutator methods and a smoothing property of the Schrödinger evolution group. *Math. Z.*, **191**, 53–59.

KARAKASHIAN, O. & MAKRIDAKIS, C. (1998) A space-time finite element method for the nonlinear Schrödinger equation: the discontinuous Galerkin method. *Math. Comput.*, **67**, 479–499.

KURTINAITIS, A. & IVANAUSKAS, F. (2004) Finite difference solution methods for a system of the nonlinear Schrödinger equations. *Nonlinear Anal. Model. Control.*, **9**, 247–258.

LEVIN, F. S. & SHERTZER, J. (1985) Finite-element solution of the Schrödinger equation for the helium ground state. *Phys. Rev. A Gen. Phys.*, **32**, 3285–3290.

LIU, H. (2015) Optimal error estimates of the direct discontinuous Galerkin method for convection–diffusion equations. *Math. Comp.*, **84**, 2263–2295.

LIU, H. & PLOYMAKLAM, N. (2015) A local discontinuous Galerkin method for the Burgers–Poisson equation. *Numer. Math.*, **129**, 321–351.

LIU, H. & YAN, J. (2009) The direct discontinuous Galerkin (DDG) methods for diffusion problems. *SIAM J. Numer. Anal.*, **47**, 675–698.

LIU, H. & YAN, J. (2010) The direct discontinuous Galerkin (DDG) method for diffusion with interface corrections. *Commun. Comput. Phys.*, **8**, 541–564.

LIU, H. & YI, N.-Y. (2016) A Hamiltonian preserving discontinuous Galerkin method for the generalized Korteweg–de Vries equation. *J. Comput. Phys.*, **321**, 776–796.

LU, T., CAI, W. & ZHANG, P. W. (2004) Conservative local discontinuous Galerkin methods for time dependent Schrödinger equation. *Int. J. Numer. Anal. Mod.*, **2**, 75–84.

LU, W.Y., HUANG, Y. Q. & LIU, H. (2015) Mass preserving direct discontinuous Galerkin methods for Schrödinger equations. *J. Comp. Phys.*, **282**, 210–226.

MENG, X., SHU, C.-W. & WU, B. (2016) Optimal error estimates for discontinuous Galerkin methods based on upwind-biased fluxes for linear hyperbolic equations. *Math. Comp.*, **85**, 1225–1261.

PATHRIA, D. & MORRIS, J. L. (1990) Pseudo-spectral solution of nonlinear Schrödinger equations. *J. Comput. Phys.*, **87**, 108–125.

RIVIÈRE, B. & WHEELER, M. F. (2000) A discontinuous Galerkin method applied to nonlinear parabolic equations. *Discontinuous Galerkin Methods: Theory, Computation and Applications* (B. Cockburn, G. Karniadakis & C.-W. Shu eds). Lecture Notes in Computational Science and Engineering, vol. 11. Berlin: Springer, pp. 231–244.

ROBINSON, M. P. (1991) Numerical solution of Schrödinger equations using finite element methods. *Ph.D. Thesis*, University of Kentucky, USA.

TAHA, T. R. & ABLOWITZ, M. I. (1984) Analytical and numerical aspects of certain nonlinear evolution equations. II. Numerical, nonlinear Schrödinger equation. *J. Comput. Phys.*, **55**, 203–230.

WARBURTON, T. & HESTHAVEN, J. S. (2003) On the constants in hp -finite element trace inequalities. *Comput. Methods Appl. Mech. Eng.*, **192**, 2765–2773.

XU, Y. & SHU, C. W. (2005) Local discontinuous Galerkin methods for nonlinear Schrödinger equations. *J. Comput. Phys.*, **205**, 72–97.

XU, Y. & SHU, C. W. (2012) Optimal error estimates of the semidiscrete local discontinuous Galerkin methods for higher order wave equations. *SIAM. J. Numer. Anal.*, **50**, 72–104.

YI, N.-Y. & LIU, H. (2018) An energy conserving discontinuous Galerkin method for a nonlinear variational wave equation. *Comm. Comput. Phys.*, **23**, 747–772.

ZHANG, R. P., YU, X. J. & FENG, T. (2012a) Solving coupled nonlinear Schrödinger equations via a direct discontinuous Galerkin method. *Chin. Phys. B.*, **21**, 30202-1–30202-5.

ZHANG, R. P., YU, X. J. & ZHAO, G. Z. (2012b) A direct discontinuous Galerkin method for nonlinear Schrödinger equation. *Chinese J. Comput. Phys.*, **29**, 175–182 (in Chinese).